2021-01-0678 Published 06 Apr 2021

Response Characteristics of an Amperometric NOx-O2 Sensor at Non diffusion-Rate-Determining Conditions

Masoud Aliramezani and Charles Koch University of Alberta

Citation: Aliramezani, M. and Koch, C., "Response Characteristics of an Amperometric NOx-O2 Sensor at Non diffusion-Rate-Determining Conditions," SAE Technical Paper 2021-01-0678, 2021, doi:10.4271/2021-01-0678.

Abstract

Experimental results are combined with a physical understanding of an amperometric NO_x-O_2 sensor to study the effect of three main operating parameters on the sensor behavior in non diffusion-rate-determining operating conditions. The sensor response to NO_x concentration is examined over a range of sensor operating temperatures, reference cell potentials, and second sensing cell potentials. The results show that the sensor sensitivity increases gradually with the sensing cell voltage while the sensor output is almost linearly dependent on NO_x concentration for cell voltages higher than ≈ 0.25 V. The results also reveal that reducing the reference cell potential from the typical cell potential (0.42 V) reduces the sensor cross-sensitivity to O_2 particularly at high NO_x concentrations (>600 [ppm]). The results of this work provide a better understanding of the sensor behavior at different operating conditions which can be used to design new accurate sensors with different sensitivities to a variety of species in the exhaust gas. This improved understanding of the sensor has the potential to remove cross-sensitivity for emission measurements of gases containing NOx and other species in the exhaust gas such as ammonia and unburned hydrocarbons.

Introduction

Stringent regulations on exhaust gas emissions reduction have been implemented all around the world [1, 2] and the automotive industry is expecting stricter regulations in the future [3].

Real-time emission measurement is a promising tool to meet the upcoming automotive market demands as well as the strict real driving emission (RDE) regulations [4]. The fast response, small size, and reliability of solid-state electrochemical sensors has made them ideal for the automotive industry [5, 6]. Amperometric sensors are a type of solid state electrochemical sensors that are used increasingly in commercial combustion engines to meet the stringent emission regulations [7, 8]. Their signal is used as an input to engine control strategies that reduce engine emissions and increase the combustion efficiency [9, 10]. Amperometric sensors generate an output that is linearly dependant on the concentration of the measuring gas, which makes these sensors easy to calibrate and suitable for detecting high gas concentrations [11, 12]. Amperometric O_2 sensors are used as wide-band lambda sensors in Diesel and Spark Ignition (SI) engines [13] and amperometric NO_x sensors are used for closed loop control of NO_x reduction aftertreatment systems such as Selective Catalytic Reduction (SCR) [14]. However, the cross-sensitivity of these sensors to the other species in the exhaust gas such as ammonia and hydrocarbons affects their accuracy and performance [15]. A fundamental understanding of the effect of the sensor operating conditions on the sensor sensitivity to NO_x provides insight into removing cross-sensitivity of the NO_x-O_2 sensor to the other species in the exhaust gas such as ammonia and unburned hydrocarbons.

The effect of main operating conditions of an amperometric NO_x-O_2 sensor on sensor sensitivity to NO_x and the linearity of the sensor response to NO_x concentration is studied in this work. Determining the range of sensor operating conditions that result in a linear input-output relationship is essential to guarantee that the sensor works in diffusion-rate-determining condition. As long this conditions is fulfilled, the sensor cross sensitivity to any other gas species can be modified by changing the sensor operating conditions without any adverse side effect on the sensor performance. The results of this study, provide insight into which operating range of an amperometric NO_x-O_2 sensor can be used to reduce or remove the sensor cross-sensitivity to other exhaust gas species.

Sensor Working Principle

An amperometric NO_x-O_2 sensor consists of two sensing chambers and one reference chamber as schematically shown in Figure 1. The sample gas first diffuses through the sensor diffusion barrier into the first chamber (O_2 sensing chamber). All the O_2 molecules are reduced in the first chamber through an electrochemical cell with a pumping current, typically, proportional to the oxygen concentration in the sample gas. In addition to O_2 reduction in the first chamber, NO_2 is also

FIGURE 1 Working principle of an amperometric NO_x sensor. This figure is adapted from [17]

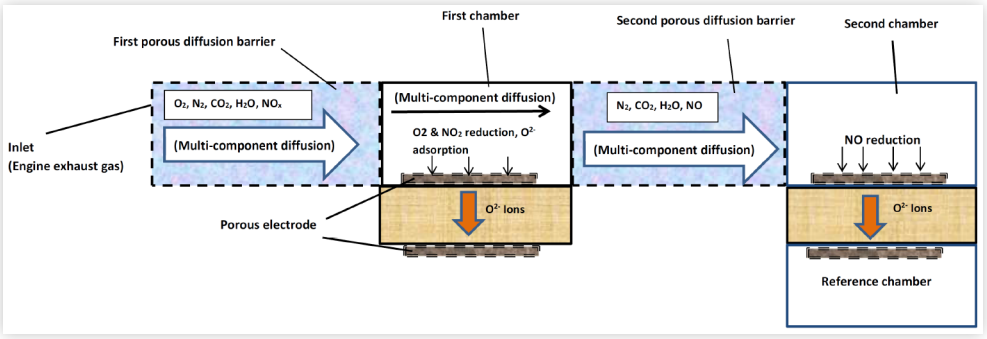

reduced to NO and the NO molecules diffuse through the second diffusion barrier into the NO_x sensing chamber. In the second chamber, NO is completely reduced by an electrochemical cell with a pumping current that is typically proportional to the total NO_x (NO_2 and NO) concentration in the sample gas [16]. More detailed information about the sensor working principle is available in [17].

The Role of Electrochemical Cell Potential

A typical cell current vs cell voltage response of an amperometric sensor is shown in Figure 2. When the cell voltage is lower than the open-circuit (zero-current) potential, the reverse reaction (oxidation) takes place causing a negative cell current. When the cell voltage is above the open-circuit potential and less than the limiting current voltage, the sensor output is a function of the reduction rate of species on the sensing electrode. This reduction rate is defined by the activation polarization and the Ohmic effect. As the cell voltage increases further, the cell current finally reaches a saturation level determined by the diffusion rate of reducible species (in this case, O_2 and NO_x) into the chamber (region II of Figure 2). In region II the pumping rate of (O^{2-}) ions from the cell has reached its maximum level since all available reducible molecules are being reduced on the sensing electrode as soon as they reach the electrode surface. A further increase in the cell voltage, causes a further increase in the cell current as illustrated in region III of Figure 2. This can potentially damage the sensor electrolyte.

The O_2 sensing cell potential, V_{P1}, affects the mole fraction of NO inside the first chamber, $x_{NO,fc}$, as [17]:

$$V_{P1} = \underbrace{E^o_{fc} + \frac{\Delta S_{ox-red,fc}}{2F}\left(T - T_o\right) - \frac{\bar{R}T}{2F} ln\left(\frac{x_{NO,env}}{x_{NO,fc}}\right)}_{E_N} - \eta_a \quad (1)$$

where, ΔS_{ox-red} is the change in entropy of *products* − *reactants* at the operating temperature (the index *fc* stands for the first chamber) and E^o_{fc} is the open-circuit potential at the standard state (1 atm; 298.15 K) while $x_{NO,env}$ and $x_{NO,fc}$ are

FIGURE 2 Typical electrode current vs potential relation

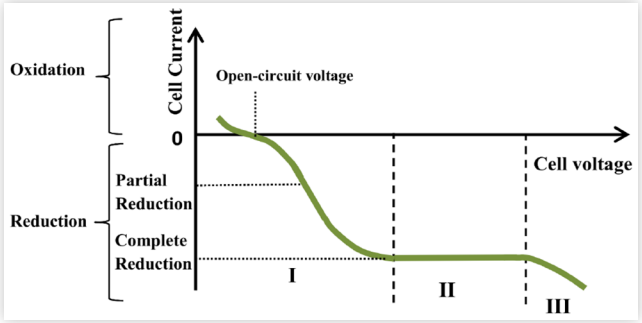

the molar fraction of NO in the sample gas and in the first chamber respectively. On the other hand, the NO_x sensing cell potential, V_{P2}, affects the mole fraction of NO inside the second chamber, $x_{NO,sc}$, as follows [17]:

$$V_{P2} = \underbrace{E^o_{sc} + \frac{\Delta S_{ox-red,sc}}{2F}\left(T - T_o\right) - \frac{\bar{R}T}{2F} ln\left(\frac{x^{0.5}_{O_2,rc} x^{0.5}_{N_2,rc}}{x_{NO,sc}}\right)}_{E_N} - \eta_\Omega - \eta_{ac} \quad (2)$$

where, $x_{O2,rc}$ and $x_{N2,rc}$ are the mole fraction of O_2 and N_2 in the reference chamber. The mole fraction of NO in the second chamber is $x_{NO,sc}$.

THE ROLE OF SENSOR TEMPERATURE At typical operation of an amperometric sensor, the sensing cell potential is high enough so that the pumping current is equal to the limiting current determined by diffusion of species through the barriers (region II). Therefore, for a typical sensor cell potential, an increase in the sensor temperature will affect the sensor output, by affecting the diffusive flow of species into the sensing chambers [18]. According to the normal diffusion mechanism, the diffusion coefficient, D_n, increases with the sensor temperature as [18]:

$$D_n \propto T^{1.75} \quad (3)$$

However, when diffusion is not the only rate determining factor for reduction of species over the sensor electrodes, the sensor temperature will affect the sensor output current in a more complex way as [17]:

$$I_P = A_e i^o_P \left(\frac{x}{x^o}\right)^\gamma \left[exp\left(\frac{\alpha_a F}{\bar{R}T}\eta_{ac}\right) - exp\left(\frac{-\alpha_c F}{\bar{R}T}\eta_{ac}\right)\right] \quad (4)$$

TABLE 1 Engine operating conditions and NO_x concentration in the exhaust gas. *Water condensation inside the sample lines may have affected the concentration of water measured by the FTIR. **The stoichimetric air/fuel ratio is changed to change the level of NO_x emission in the SI engine

Engine	Engine speed [rpm]	BMEP [bar]	NO_x[ppm]	CO_2 [%]	H_2O*[%]	CO [ppm]
SI**	2000	6.6982	468, 818, 1124, 1373, 1748	-	-	-
Diesel	2500	1.1358	103	2.82	3.12	2.82
Diesel	2000	3.7862	175	4.00	3.21	154
Diesel	1500	7.5723	368	6.50	3.24	177

where, A_e, i_P^o, x and x^o are the sensing electrode area, the reference exchange current density, the mole fraction of reduced species inside the chamber and the reference mole fraction of the reduced species in the sensing chamber respectively, while α_a and α_c are the charge transfer coefficient of anode and cathode respectively. The overpotential η_{ac} is defined as $\eta_{ac} = V_P - E_{OC}$, where V_P and E_{OC} are the potential and the open circuit (zero-current) potential of the sensing cell.

Experimental Setup

A fully-controlled sensor test rig was used to expose the sensor to a prepared gas mixture with different concentrations of species. The test rig consists of six externally controlled 2-way valves, connected to gas cylinders filled to known concentrations, three 3-way valves, four humidifying tanks and six CCR MKS-GE50A mass flow controllers. All of the setup actuators are controlled externally by the test rig control computer. More details about the sensor test rig is available in [17]. To also study the sensor behavior in real engine conditions over a wide range of exhaust gas species concentrations, the sensor was mounted upstream of the engine aftertreatment systems to measure the engine raw emissions in the exhaust pipe. The two engines tested were a four cylinder medium duty Tier III diesel engine (Cummins QSB 4.5 160) and a four cylinder port injection spark ignition (SI) engine fueled with natural gas (GM Vortec 3000). The tests were carried out at different engine operating conditions resulting in different engine out NO_x concentrations in the exhaust gas which are listed in Table 1. A production ECM NO_x sensor (P/N: 06-05) was used in the experiments. The sensor parameters and operating condition were changed using the sensor control module (*ECM-NOxCANt* P/N: 02-07) connected to a computer via *Kvaser Light HS* CAN interface. A FTIR analyser (*MultiGas 2030*) was used to validate the NO_x sensor measurement and to measure the concentration of other species in the exhaust gas. The FTIR analyser was connected to the diesel engine exhaust pipe, upstream of the catalysts to measure the engine raw emissions. The sample exhaust gas passes through two Heated Filters (*Flexotherm*) connected with Heated Sample Lines (*Flexotherm*) heated to 191°C to minimize water vapor condensation in the sample gas [19]. It is assumed that changing the sensor operating conditions only affects the chemical and electrochemical reactions inside the sensor and on the electrodes without causing electrolyte decomposition.

Results and Discussion

THE EFFECT OF SENSOR TEMPERATURE The sensor response is studied at three sensor temperatures and four diesel engine operating conditions. The engine emissions concentrations measured by the FTIR system are listed in Table 1. The sensor temperatures selected for this study are close to the typical design sensor operating temperature (1023 K) and are controlled by a built in heater located inside the sensor ceramic layers. Decreasing the sensor temperature to lower than the sensor design temperature, reduces the diffusion coefficient of NO through the sensor diffusion barriers according to Eqn. (3). The typical sensing cell potential ($VP_1 \approx 0.4$ V) is high enough to partly reduce NO on the Pt-Au electrodes in the first chamber [17] as shown in Figure 2. Thus reducing the sensor temperature reduces the reduction rate of NO inside the first chamber according to Eqn. (1) which increases the molar fraction of NO inside the first chamber causing an increase in the molar flow rate of NO, according to Fick's law [20], to the second chamber. Increasing the sensor temperature increases the diffusion rate of NO through the sensor barriers and reduction rate of NO in the first chamber. At a sensor temperature of 1080 K, the effect of temperature increase on NO reduction in the first chamber outweighs its effect on the diffusion rate. As a result, less NO is delivered to the NO_x sensing chamber which consequently reduces the pumping current of NO in the NO_x sensing chamber as shown in Figure 3a and Table 2. The linearity of sensor response is also reduced up to 1.2 % at the high sensor temperature (1080 K) as depicted in Table 2 which adversely affects the sensor accuracy, when sensor linearity is assumed, particularly at high NO_x concentrations.

THE EFFECT OF REFERENCE CELL POTENTIAL The reference cell potential, V_S, represents the partial pressure of O_2 inside the O_2 sensing chamber. The mole fraction of O_2 inside the O_2 sensing chamber decreases by increasing the reference cell potential, according to Eqn. (4). Therefore, by reducing the set point value of the reference cell potential, the O_2 concentration increases in the first chamber. Four values of V_S are selected as listed in Table 3. This can lead to an offset in the pumping current of the NO_x sensing chamber, particularly at low NO_x concentrations as shown in Figure 3b. Apart from the effect of reference cell potential on the NO_x sensor response, it also affects the sensor cross-sensitivity to O_2. The presence of O_2 in the sample gas has a more significant effect on the sensor response slope at $V_S = 0.42$ V than $V_S = 0.35$ V as shown in Figure 3b and Table 3, which reveals that the NO_x sensor response has a higher cross-sensitivity to O_2 at

FIGURE 3 (a) The effect of sensor temperature on sensor output I_{P2} as a function of NO_x by examining the sensor sensitivity (slope) and linearity. (b) The effect of reference potential (*VS*) resulting in the presence of O_2 on sensor output I_{P2} as a function of NO_x by examining the sensor sensitivity (slope) and sensor linearity. Cases are explained in Table 3

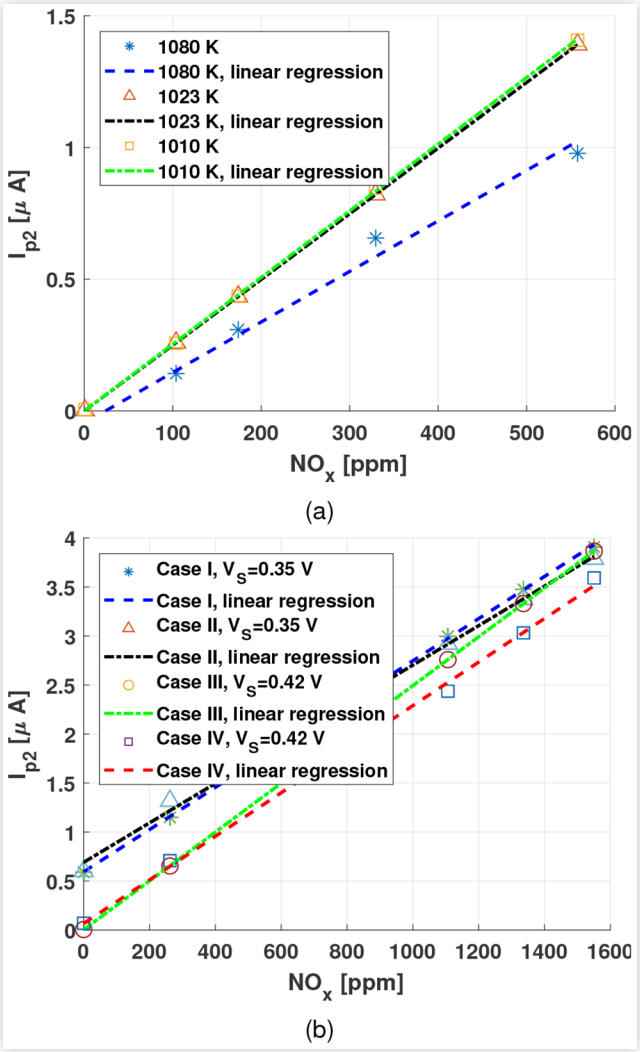

V_S = 0.42 V. This effect is mainly due to the difference between the corresponding O_2 sensing cell potential, V_{p1}, as illustrated in Figure 4 with the cases described in Table 3.

THE EFFECT OF SECOND (NO_x SENSING) CELL POTENTIAL The most important factor that affects an amperometric NO_x sensor performance is the potential of the NO_x sensing cell, V_{P2} [17]. To better understand the effect of NO_x sensing cell potential on the sensor sensitivity to NO_x, the slope of the sensor output vs NO_x concentration is calculated at different cell potentials and the experimental results are shown in Figure 5a along with the corresponding linear regression plot at each NO_x sensing cell potential. The details of each case indicated in Figure 5a are listed in Table 4.

The sensitivity of the sensor output to NO_x generally increases with the NO_x sensing cell voltage (V_{P2}) since the reduction rate of NO increases with increasing the NO_x sensing cell potential, according to Eqn. (2). Therefore, the

FIGURE 4 The effect of reference potential and presence of O_2 on the O_2 sensing chamber. Cases are explained in Table 3

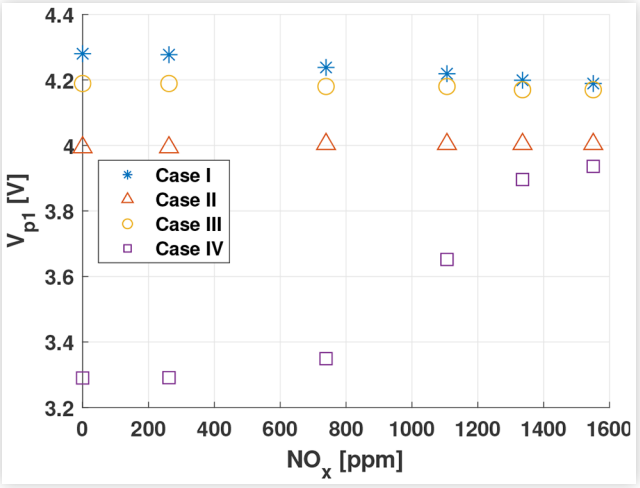

TABLE 2 Linearity of I_{P2} vs NO_x as a function of sensor temperature - from Figure 3a

Case	Sensor temperature [K]	R^2	Slope
1	1010	0.9998	0.002531
2	1023	0.9999	0.002493
3	1080	0.98751	0.001918

TABLE 3 Reference cell potential (RCP) and linear fit characteristics of the cases shown in Figure 3b

Case	RCP [V]	With O_2?	R^2	Slope
I	0.35	YES	0.99986	0.0022
II	0.35	NO	0.99752	0.0020
III	0.42	YES	0.99999	0.0025
IV	0.42	NO	0.99786	0.00222

TABLE 4 NO_x sensing cell potential (SCP) and linear fit characteristics of the cases shown in Figure 5a

Case	NO_x SCP [V]	R^2	Slope
1	0.138	0.0467	−2.453e−5
2	0.170	0.7268	1.48e−4
3	0.189	0.9218	2.20e−4
4	0.199	0.9773	2.41e−4
5	0.250	0.9946	5.98e−4
6	0.343	0.9986	1.01e−3
7	0.447	0.9999	1.20e−3

mole fraction of NO inside the NO_x sensing chamber decreases according to Eqn. (2) which causes an increase in the pumping current. The linearity of the sensor output vs NO_x concentration also increases with the cell voltage. This trend is also shown in Figure 5b. One aspect to emphasize in Figure 5b, is the different effect of the NO_x sensing cell potential on the sensor response linearity (linear regression R^2) and the sensor

FIGURE 5 (a) I_{p2} vs NO_x concentration at different NO_x sensing cell voltages - from V_{P2}= 0.138 V to V_{P2}= 0.447 V - (see Table 4). (b) The effect of NO_x sensing cell voltage on sensitivity and linearity of the NO_x sensor

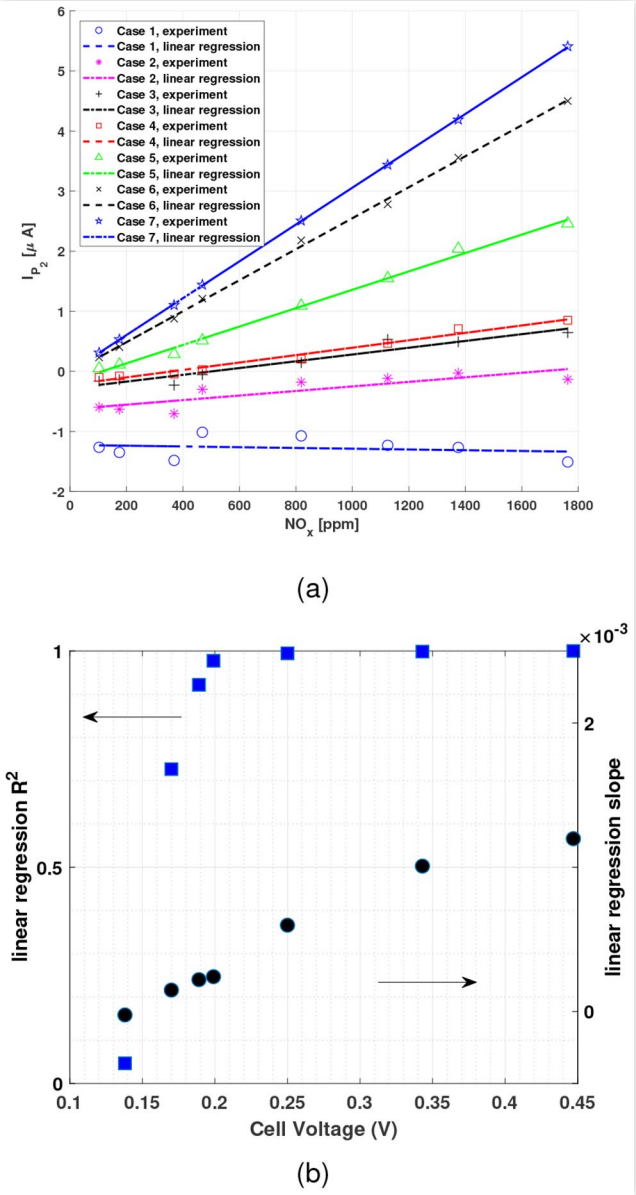

sensitivity to NO_x concentration (linear regression slope). The sensor sensitivity increases gradually with the cell potential while the linearity of the sensor dramatically (>95 %) increases at sensor potential ≈ 0.25 V and remains higher than 0.995 for V_{P2}> 0.25 V. In other words, although the sensor sensitivity to NO_x gradually increases with the cell potential for cell potentials higher than 0.25 V, the sensor output is almost linear at any points within this range. This behavior can be used to design accurate sensors with different sensitivities to other species such as NH_3 and unburned hydrocarbons as it provides an insight into the sensor sensitivity and operating range. As a case in point, an innovative approach was proposed by the authors in [21] to ensure diffusion-rate-determining operation of an amperometric sensor which resulted in a reliable method to measure the concentration of hydrocarbons (propane) inside gas streams. The sensor operating parameters can significantly affect the sensor sensitivity to a specie, as shown in this work. Desired sensor performance is achieved when the sensor sensitivity to a desired specie is sufficient and the sensor response vs concentration of desired specie is linear. Simultaneously, the sensor cross sensitivity to the other species should be minimized or at least be predictable. The results of this work provide an insight into the operating region of an amperometric NO_x sensor with sufficient sensitivity and linearity to NO_x.

Conclusions

The paper continues our previous studies on the performance of amperometric NO_x sensors [16, 17] by investigating their performance at non diffusion-rate-determining conditions.

The effect of these main operating parameters of an amperometric NO_x sensor were understood based on a phenomenological model. The experimental results show that:

- The sensor sensitivity to NO_x decreases by increasing the sensor temperature. Increasing the sensor temperature to more than the sensor design temperature (1023 K), reduces the sensor response linearity to NO_x concentration.
- Reducing the reference cell potential from the typical cell potential (0.42 V) increases the NO_x sensor response offset at low NO_x concentrations but also reduces the sensor cross-sensitivity to O_2 particularly at high NO_x concentrations (>600 [ppm]).
- The sensor sensitivity gradually increases as the NO_x sensing cell potential increases while the sensor output becomes almost linearly dependent on NO_x concentration for cell potentials higher than ≈ 0.25 V.

This improved understanding of the sensor has the potential to remove cross-sensitivity for emission measurements of gases containing NO_x and other species in the exhaust gas such as unburned hydrocarbons and NH_3 by providing an insight into the sensor sensitivity and operating range.

Acknowledgment

This work has been partially supported by the Natural Sciences and Engineering Research Council of Canada (grant number 2016-04646) and Canada First Research Excellence Fund.

References

1. Rastogi, A., Rajan, A.V., and Mukherjee, M., "A Review of Vehicular Pollution and Control Measures in India," . In: *Advances in Health and Environment Safety.* (Springer, 2018), 237-245.

2. Liu, Z., Hao, H., Cheng, X., and Zhao, F., "Critical Issues of Energy Efficient and New Energy Vehicles Development in China," *Energy Policy* 115:92-97, 2018.
3. Tang, W., Siani, A., Chen, F., and Chen, B., "On Developing Advanced Catalysts Systems to Meet China New Regulations," in *WCX SAE World Congress Experience*, SAE International, April 2019.
4. Hooftman, N., Messagie, M., Van Mierlo, J., and Coosemans, T., "A Review of the European Passenger Car Regulations - Real Driving Emissions vs Local Air Quality," *Renewable and Sustainable Energy Reviews* 86:1-21, 2018.
5. Mello, H.J.N.P.D. and Mulato, M., "Influence of Galvano-Static Electrodeposition Parameters on the Structure-Property Relationships of Polyaniline Thin Films and their Use as Potentiometric and Optical pH Sensors," *Thin Solid Films* 656:14-21, 2018.
6. Aliramezani, M., Norouzi, A., and Koch, C.R., "A Grey-Box Machine Learning Based Model of an Electrochemical Gas Sensor," *Sensors and Actuators B: Chemical* 321:128414, 2020.
7. Ritter, T., Hagen, G., Lattus, J., and Moos, R., "Solid State Mixed-Potential Sensors as Direct Conversion Sensors for Automotive Catalysts," *Sensors and Actuators B: Chemical*, 2017.
8. Qi, G. and Perry, K.L., "NOx Sensor Calibration and Application in Lean NOx Trap Aftertreat Systems," US Patent 9,863,922, 2018.
9. Salehi, R., Martz, J., Stefanopoulou, A., Vernham, B., Uppalapati, L., and Prashant Baliga, B.. Decentralized Feedback Control of Pumping Losses and NOx Emissions in Diesel Engines. *Journal of Engineering for Gas Turbines and Power*, 140(10), 06 2018. 102810.
10. Aliramezani, M., Norouzi, A., Koch, C.R., and Hayes, R.E.. "A Control Oriented Diesel Engine NOx Emission Model for on Board Diagnostics and Engine Control with Sensor Feedback," in *Proceedings of Combustion Institute - Canadian Section*, 2019.
11. Ritter, T., Seibel, M., Hofmann, F., Weibel, M., and Moos, R., "Simulation of a NOx Sensor for Model-Based Control of Exhaust Aftertreatment Systems," *Topics in Catalysis*1-7, 2018.
12. Aliramezani, M., Koch, C.R., and Patrick, R., "A Variable-Potential Amperometric Hydrocarbon Sensor," *IEEE Sensors Journal.*, 2019.
13. Regitz, S. and Collings, N., "Fast Response Air-to-Fuel Ratio Measurements Using a Novel Device Based on a Wide Band Lambda Sensor," *Measurement Science and Technology* 19(7):075201, 2008.
14. Bonfils, A., Creff, Y., Lepreux, O., and Petit, N., "Closed-Loop Control of a SCR System Using a NOx Sensor Cross-Sensitive to NH3," *Journal of Process Control* 24(2):368-378, 2014.
15. Aliramezani, M., Koch, C.R., and Hayes, R.E., "Estimating Tailpipe NOx Concentration Using a Dynamic NOx/ammonia Cross Sensitivity Model Coupled to a Three State Control Oriented SCR Model," *IFAC-PapersOnLine* 49(11):8-13, 2016.
16. Aliramezani, M., Koch, C.R., Hayes, R.E., and Patrick, R., "Amperometric Solid Electrolyte NOx Sensors - the Effect of Temperature and Diffusion Mechanisms," *Solid State Ionics* 313(Supplement C):7-13, 2017.
17. Aliramezani, M., Koch, C.R., Secanell, M., Hayes, R.E., and Patrick, R., "An Electrochemical Model of an Amperometric NOx Sensor," *Sensors and Actuators B* 290:302-311, 2019.
18. Aliramezani, M., Koch, C.R., and Patrick, R., "Phenomenological Model of a Solid Electrolyte NOx and O2 Sensor Using Temperature Perturbation for On-Board Diagnostics," *Solid State Ionics* 321:62-68, 2018.
19. Klikach, R., "Investigation and Analysis of RCCI using NVO on a Converted Spark Ignition Engine," Master's Thesis, 2018.
20. Welty, J.R., Wicks, C.E., Rorrer, G., and Wilson, R.E., *Fundamentals of Momentum, Heat, and Mass Transfer* (John Wiley & Sons, 2009).
21. Aliramezani, M. and Koch, C.R., "A Variable-Potential Limiting-Current-Type Amperometric Hydrocarbon Sensor," *IEEE Sensors Journal*, 2019.

ISSN 0148-7191